STM JOURNALS

Journal of
Polymer & Composites

ISSN: 2321-2810 (Online)
ISSN: 2321-8525 (Print)
Volume 12, Special Issue 4, 2024
DOI (Journal): 10.37591/JoPC

http://engineeringjournals.stmjournals.in/index.php/JoPC/index

Research JoPC

Influence of Center Cut Geometry and Power Law Index on the Free Vibration of Functionally Graded Shells

Ramu Inala[1*], Chandra Sekhar J[2], Venu M[3], Battina N. Malleswararao[4], Manikanta NVV[5]

Abstract

This study explores the influence of power law variations and center cut geometries on the vibrational characteristics of functionally graded material (FGM) shells using finite element analysis (FEA). Stainless steel-alumina oxide (Al2O3) composites serve as the FGM, offering a unique blend of ceramic heat resistance and metallic toughness. Power law functions within APDL tailor material properties across the shell thickness. The research investigates vibrations under various boundary conditions (CCCC, CCFF, CFFF) for FGM shells with distinct center cuts (rectangular, circular, square). Key findings reveal a strong correlation between center cut geometry and natural frequencies. Square cuts induce the highest frequencies, while circular cuts exhibit the lowest. Rectangular cuts fall between these extremes. This emphasizes the center cut's role in modulating vibrations. Furthermore, increasing the power law index systematically lowers frequencies across all cut sections. Boundary conditions significantly impact bending and torsional frequencies, with all sides clamped configurations yielding the highest values. This work provides valuable insights into tailoring vibration characteristics of FGM shells for diverse engineering applications.

Keywords: Functionally graded materials, Shell, Centre Cuts, Vibration, Finite element method**.**

INTRODUCTION

This research on the vibration characteristics of functionally graded material (FGM) shells, with a specific focus on configurations containing center cuts. FGMs, known for their tailorable material properties, offer promising advantages in various engineering applications introduced by Naebe and Shirvanimoghaddam [1]. Several studies have investigated the application of FEM (Finite Element Method) to analyze the dynamic behavior of FGM structures. Ramu and Mohanty [2, 3] employed FEM for modal and buckling analyses of FGM plates under various boundary conditions. Rao et al. [4] explored FEM modeling and analysis of functionally graded composite shell structures. Sharma et al. [5] utilized FEM for harmonic analysis of FGM plates, highlighting its effectiveness in vibration analysis. Research on the free vibration of FGM structures is also relevant. Ghassabi [6] analyzed free vibration in functionally graded rectangular nano-plates, while Ramu and Mohanty [7] investigated free vibration and dynamic stability of FGM plates on elastic foundations. These studies demonstrate the importance of analyzing vibration characteristics in FGMs to ensure structural integrity.

***Author for Correspondence**
Ramu Inala

[1,2,3,5]Assistant Professor, Mechanical Engineering, Vishnu Institute of Technology, Bhimavaram, Andhra Pradesh, India.
[4]Associate Profesor Mechanical Engineering, Shri Vishnu Engineering College for Women, Bhimavaram, Andhra Pradesh, India..

Received Date: May 01, 2024
Accepted Date: May 31, 2024
Published Date: July 18, 2024

Citation Ramu Inala , Chandra Sekhar J, Venu M, Battina N. Malleswararao, Manikanta NVV. Influence of Center Cut Geometry and Power Law Index on the Free Vibration of Functionally Graded Shells . Journal of Polymer & Composites. 2024; 12(Special Issue 4): S194–S209.

The introduction of center cuts in structures presents an additional layer of complexity in vibration analysis. Bhandari and Purohit [8] performed a study on functionally graded material plates experiencing transverse loads, considering different boundary conditions. Alif Ngimbi Diambu and Mehmet Çevik [9, 10]

performed finite element analyses on functionally graded plates, covering both general and vibration-specific studies. Tawakol [11] investigated stress concentrations in functionally graded plates containing elliptical holes subjected to biaxial loads. Inala Ramu [12] explored how hygrothermal conditions and functionally graded materials impact the natural frequency and parametric instability of plates. Merdaci et al. [13] examined the free vibration behavior of ceramic-metal functionally graded rectangular solar plates with porosities, utilizing high-order shear theory and investigating plates made of (Al/Al2O3) and (Al/ZrO2). Liew et al. [14] employed the discrete Ritz method to analyze free vibration of rectangular plates with central cut-outs. Kalita and Haldar [15] conducted a similar analysis using FEM for rectangular plates with central cutouts. Merneedi et al. [16] investigated free vibration of rectangular plates with multiple cut-outs, demonstrating the influence of cut configuration. Jadee et al. [17] further explored free vibration of isotropic plates with various cutouts using FEM, highlighting the impact of cutout design. Studies by Lee et al. [18] and Torabi and Azadi [19] employed different methods (Rayleigh-Ritz) to analyze vibration in rectangular plates with central holes, emphasizing the use of diverse techniques in this field.

The present work employs FEM to investigate the influence of power law variations and center cut geometries (regular, circular, square) on the vibration behavior of FGM shells under various boundary conditions. FEM has emerged as a powerful tool for analyzing FGMs, while various techniques have been employed to study vibration in structures with cut-outs. This work provides a foundation for further investigation into the vibration of FGM shells with center cuts under different boundary conditions and power law variations.

METHODOLOGY

Displacement Fields

Below is the provided generalized form of the displacement field:

$$u\,(x,y,z) = u_o(x,y,z) - z\frac{\partial w_o}{\partial x} + f(z)\left(\emptyset_x + \frac{\partial w_0}{\partial x}\right) \quad \text{Eq. (1)}$$

$$v\,(x,y,z) = v_o(x,y,z) - z\frac{\partial w_o}{\partial y} + f(z)\left(\emptyset_y + \frac{\partial w_0}{\partial y}\right) \quad \text{Eq. (2)}$$

$$w(x,y,z) = w_o(x,y,z) \quad \text{Eq. (3)}$$

In the analysis of shell, several symbols are used to describe the deformation and movement of a point within the plate. Displacements in the x, y, and z directions are represented by u, v, and w, respectively. However, for a specific point on the bottom surface of the plate (z = 0), we use u0, v0, and w0 to indicate its movement in those directions. Additionally, Øx and Øy represent the rotations of a tiny element within the plate about the x and y axes, respectively.

Strain Equations

In the theory of elasticity, where small strains and small rotations are assumed, the strains related to the displacement field can be determined linear strain-displacement relations (considering first-order terms in Taylor expansion). The strain field corresponding to the displacements can be described as:

$$\varepsilon_{xx} = \frac{\partial_u}{\partial_x} \quad \text{Eq. (4)}$$

$$\varepsilon_{yy} = \frac{\partial_u}{\partial_y} \quad \text{Eq. (5)}$$

$$\varepsilon_{zz} = \frac{\partial_u}{\partial_z} \quad \text{Eq. (6)}$$

$$\varepsilon_{xy} = \frac{1}{2}\left(\frac{\partial_u}{\partial_y} + \frac{\partial_v}{\partial_x}\right) \quad \text{Eq. (7)}$$

$$\varepsilon_{yz} = \frac{1}{2}\left(\frac{\partial_v}{\partial_z} + \frac{\partial_w}{\partial_y}\right) \quad \text{Eq. (8)}$$

$$\varepsilon_{xz} = \frac{1}{2}\left(\frac{\partial_u}{\partial_z} + \frac{\partial_w}{\partial_x}\right) \quad \text{Eq. (9)}$$

Power Law

Functionally Graded Materials (FGMs) are a class of materials where properties like Young's modulus (stiffness) and density are not uniform but exhibit a tailored variation throughout their thickness. This allows for a smooth transition of properties across the material, offering unique advantages in various engineering applications compared to traditional materials with constant properties. A power law relates two quantities, where a change in one (e.g., thickness) results in a proportional change in the other (e.g., material property) regardless of the initial values.

$$V_c(z) = \left(\frac{1}{2} + \frac{z}{h}\right)^n \quad \text{Eq. (10)}$$

$$V_c + V_m = 1 \quad \text{Eq. (11)}$$

$$E(z) = E_s + (E_c - E_s)V_c(z) \quad \text{Eq. (12)}$$

where, Ec= Young's modulus of ceramic
Em = Young's modulus of metal
h = Thickness of the shell
z = coordinate of a point on the shell thickness
n = power law index

GOVERNING EQUATION

The expression of kinetic energy of shell is represented below

$$T_P = \frac{1}{2}\rho h \int_0^a \int_0^b W^2 \, dx \, dy \quad \text{Eq. (13)}$$

The potential energy of shell is expressed as follow

$$V_p = \frac{1}{2}D \int_0^a \int_0^b \left[\left(\frac{\partial^2 W}{\partial x^2}\right)^2 + \left(\frac{\partial^2 W}{\partial y^2}\right)^2 + 2\vartheta\left(\frac{\partial^2 W}{\partial x^2}\frac{\partial^2 W}{\partial y^2}\right) + 2(1-\vartheta)\left(\frac{\partial^2 W}{\partial x \partial y}\right)^2\right] dxdy \quad \text{Eq. (14)}$$

The energies of kinetic and potential of a shell are expressed in terms of their mass and stiffness matrices, and their derivation proceeds as follows:

$$T_p = \frac{1}{2}\dot{p}^T M \dot{p} \quad \text{Eq. (15)}$$

$$V_p = \frac{1}{2}p^T K p \quad \text{Eq. (16)}$$

where M , K represents the mass and stiffness matrices of shell

The governing equation of motion is obtained by substituting the global displacement vector, mass matrix, and stiffness matrix of the functionally graded material (FGM) shell into the given equation.

$$[K - \omega^2 M]A = 0 \quad \text{Eq. (17)}$$

where ω natrural frequencis of the shell

Using above equations, the expressions of kinetic and potential energies in the cut section domain are derived as follows

$$T_H = \frac{1}{2}\dot{p}_h{}^T M_h \dot{p}_h \quad \text{Eq. (18)}$$

$$V_H = \frac{1}{2} p_h{}^T K_h p_h \quad \text{Eq. (19)}$$

where M_h ,K_h represents the mass and stiffness matrices of cut section domain

Hence the expressions for total kinetic and potential energies of shell with cut-outs are

$$T_{Total} = \frac{1}{2}\dot{p}^T M \dot{p} - \frac{1}{2}\dot{p}_h{}^T M_h \dot{p}_h \quad \text{Eq. (20)}$$

$$V_{total} = \frac{1}{2} p^T K p - \frac{1}{2} p_h{}^T K_h p_h \quad \text{Eq. (21)}$$

Therefore, the expressions for the total kinetic and potential energies of a shell with cut-outs can be derived by incorporating the respective mass matrix, and stiffness matrix are followed

$$T_{Total} = \frac{1}{2}\dot{p}^T M \dot{p} - \frac{1}{2}\sum_{i=1}^{n} \dot{p}^T T_{hi}{}^T M_{hi} T_{hi}\, \dot{p} = \frac{1}{2}\dot{p}^T M_r \dot{p} \quad \text{Eq. (22)}$$

$$V_{Total} = \frac{1}{2} p^T K p - \frac{1}{2}\sum_{i=1}^{n} p^T T_h{}^T K_h T_h\, p = \frac{1}{2} p^T K_r p \quad \text{Eq. (23)}$$

where M_r ,K_r represents the mass and stiffness matrices of shell with cut-outs. By incorporating the global vector, mass matrix, and stiffness matrix of the functionally graded material (FGM) shell into the preceding equation, the governing equation of motion for cut shells can be expressed as

$$[\underline{K}_r - \varpi^2 M_r]A = 0 \quad \text{Eq. (24)}$$

Here ϖ represents the natural frequencies of shell with cut sections

RESULTS AND DISCUSSIONS

Design of FG shell

This study examines how different power law indices along with different boundary conditions affect the FGM shell thickness without a cut section and with a cut section. Various thicknesses of 40 mm and 4 mm were used for the modal analysis of the FGM shell measuring 300x300 mm in length and width. Shell without cut-section and with cut-section are designed in the CATIA V5 software and the model is imported into ANSYS workbench with “iges” extension for the modal analysis. The designed models are shown in the figure 1. In this study, stainless steel and aluminum oxide (Al_2O_3) are considered. Below table 1 shows the various properties such as young’s modulus, density, and poisson's ratio.

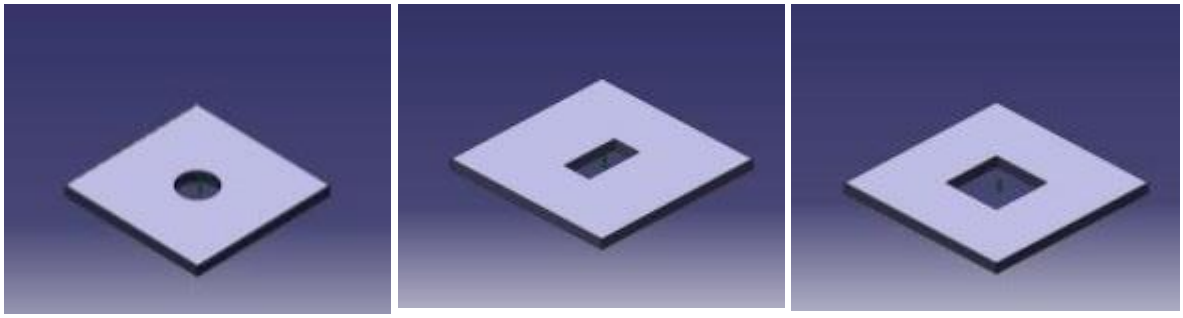

(a) with circular hole (b) with rectangular hole (c) with square hole

Figure 1. FGM shell with Centre cuts of different cross-sections

Table 1. Material properties of stainless steel and aluminum oxide.

Material	Young's Modulus (GPa)	Density (Kg/m3)	Poisson's Ratio (μ)
Stainless Steel	208	8166	0.3
Aluminum Oxide (Al_2O_3)	320	3970	0.3

Various power-law indices, including 0.5,1,2,5,10, as well as different boundary conditions, such as all sides clamped, two opposite sides clamped, and one side clamped (CFFF), are used to determine the first four natural shapes and their modes. Specifically, we will analyze its natural frequencies and mode shapes to gain insights into its structural response. This is when presented with the given boundary conditions.

FGM Shell Without Cut Section

Natural frequencies for the first four nodes of CCCC when n=1 is shown in table 2 is compared with the previous literature Alif and Mehmet [10]. From the below table, the modes of vibration of rectangular plates are notably affected by factors such as thickness, aspect ratios, and boundary conditions, particularly when all sides are clamped. Altering the thickness and aspect ratio leads to an increase in the aspect ratio and, subsequently, a decrease in the natural frequencies' modes for rectangular plates. It has been observed that, under the all sides clamped boundary condition, the frequency decreases as the aspect ratio increases.

Table 2. Comparison of first 3-modes of natural frequencies (CCCC, n=1)

Thickness	N	a/h ratio		Mode 1	Mode 2	Mode 3
40	1	7.50	Present	4272.09	7996.86	11003.02
			Alif and Mehmet [10]	4342.6	8058.2	11100
36	1	8.33	Present	3945.04	7484.94	10367.06
			Alif and Mehmet [10]	4008.8	7535.1	10450
32	1	9.38	Present	3593.87	6913.55	9645.71
			Alif and Mehmet [10]	3650.6	6952.7	9712.9
28	1	10.71	Present	3218.06	6277.43	8827.88
			Alif and Mehmet [10]	3267.7	6306.1	8879.8
24	1	12.50	Present	2817.61	5572.23	7902.66
			Alif and Mehmet [10]	2860	5591.4	7940
20	1	15.00	Present	2393.16	4795.32	6860.58
			Alif and Mehmet [10]	2428	4806.4	6884.8
16	1	18.75	Present	1946.25	3946.88	5695.85
			Alif and Mehmet [10]	1974.2	3951.9	5709.3
12	1	25.0	Present	1479.37	3031.11	4409.41
			Alif and Mehmet [10]	1500.2	3032.2	4415.3
8	1	37.5	Present	996.11	2057.25	3012.54
			Alif and Mehmet [10]	1010	2056.7	3014.3
4	1	75.0	Present	501.13	1040.22	1529.97
			Alif and Mehmet [10]	508.28	1039.9	1530.7

In investigating the natural frequencies of a FGM shell with all sides clamped under different power law index values, two specific thickness values of 40 and 20 were considered. The key observation from the figure 2 is that an increase in the power law index values led to a reduction in the first four mode natural frequencies of the FGM shell. In Figure 2, as the power law index values increased, there is a consistent downward trend in the natural frequencies of the FGM shell. Each curve represents a different mode, with the first four modes clearly showing a decrease in their respective frequencies with higher power law indices. This suggests that the composition or structure of the FGM shell, as characterized by the power law index, has a significant impact on its vibrational behavior.

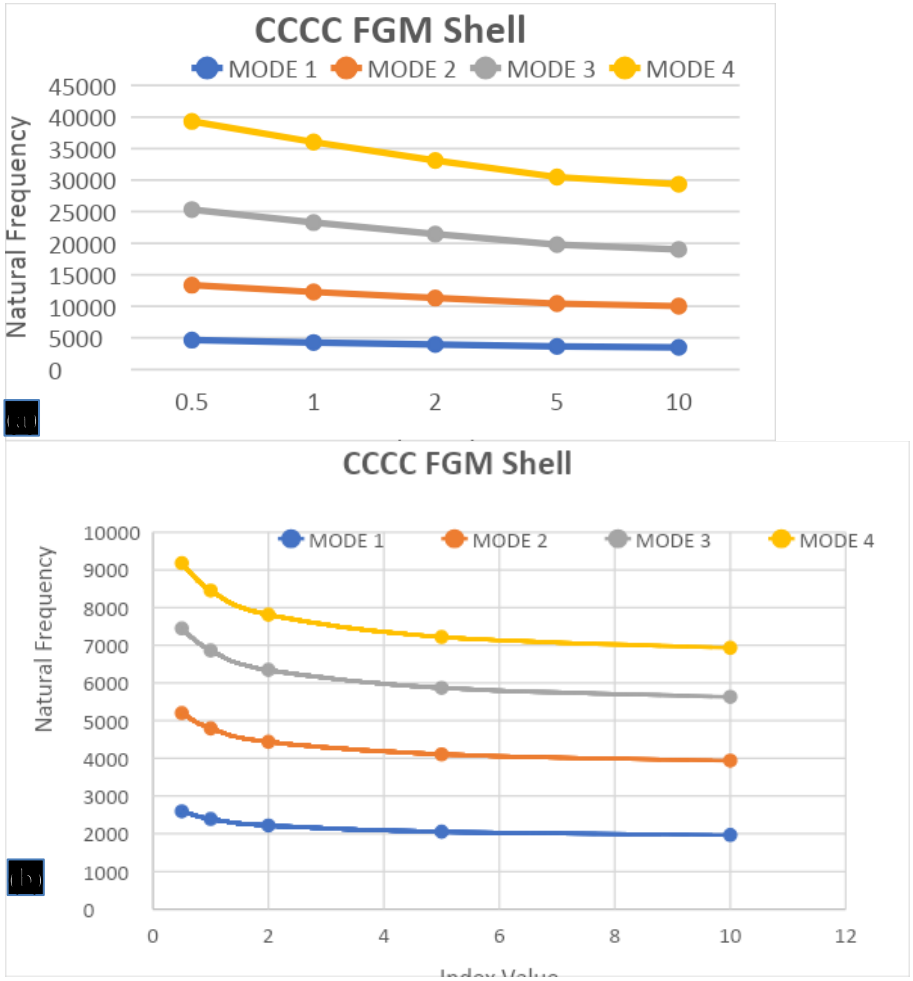

Figure 2. (a)Shell Thickness 40 mm, b) Shell Thickness 20 mm. Natural frequency versus power law index values with all side clamped boundary condition with thickness at 40 and 20

Figure 3, focusing on a thickness value of 20, further illustrates the inverse relationship between the power law index values and the natural frequencies. Similar it increases in the power law index leads to a reduction in natural frequencies across the first four modes.

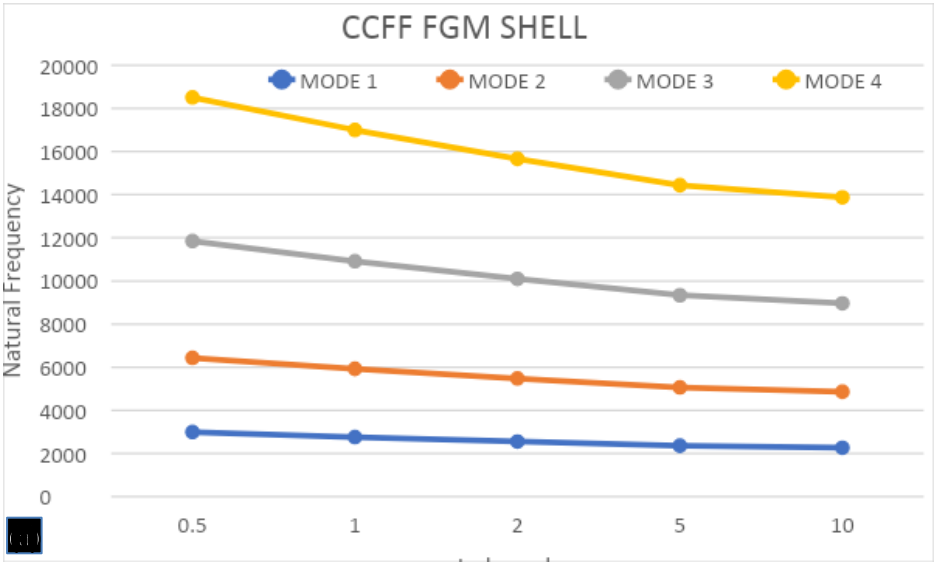

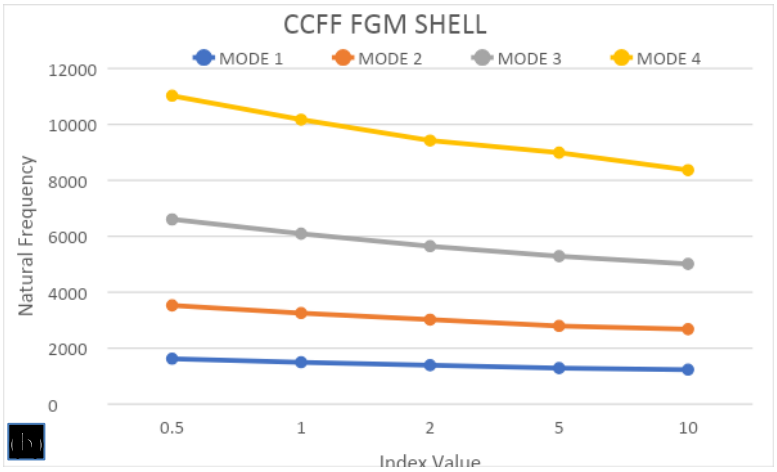

Figure 3. (a)Shell Thickness 40 mm, b) Shell Thickness 20 mm. Natural frequency versus power law index values with two side clamped and other sides free boundary condition with thickness at 40 mm and 20 mm

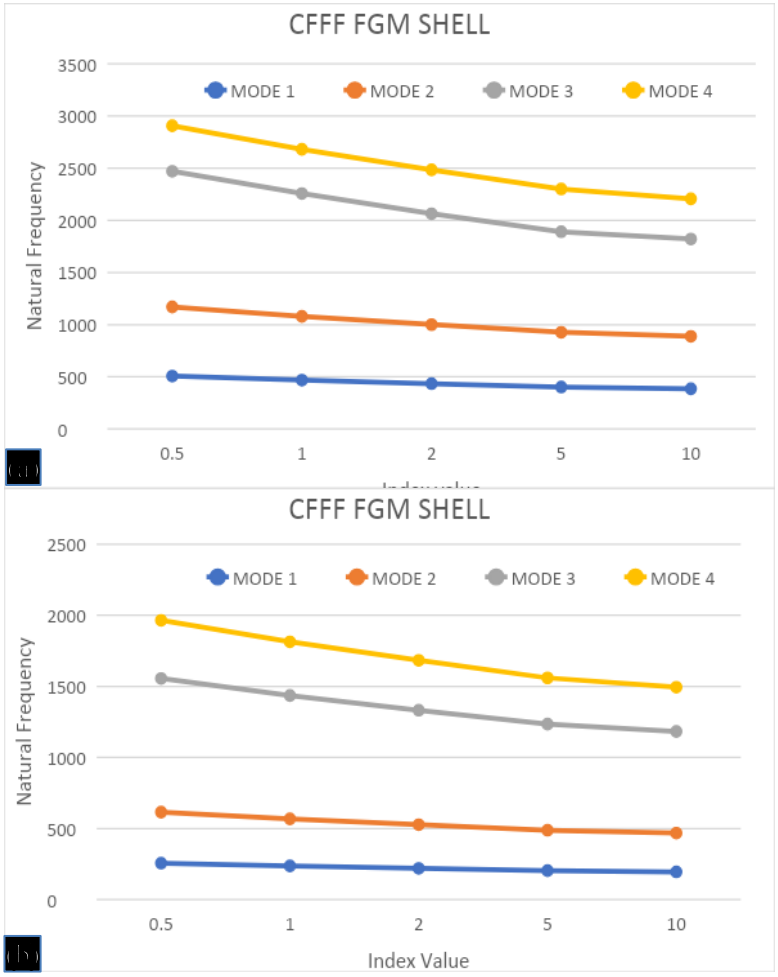

Figure 4. (a)Shell Thickness 40 mm, b) Shell Thickness 20 mm. Natural Frequencies vs. Power Law Index (One Side Clamped, Others Free) with thickness at 40 mm and 20 mm

Figure 4, the relationship between power law index values and natural frequencies is evident, particularly under the boundary condition of one side clamped and the others free. As the power law

index values increased, a consistent downward trend in natural frequencies was observed. Each curve in the figure represents a distinct mode, and the first four modes stand out with a noticeable decrease in their respective frequencies as the power law indices increase. This observation implies that alterations in the composition or structure of the FGM shell, as characterized by the power law index, exert a significant influence on its vibrational behavior under the specified boundary conditions.

The figure 4 effectively illustrates the impact of changing power law index values on the vibrational characteristics of the FGM shell. The clear trend in decreasing natural frequencies for the first four modes emphasizes the sensitivity of the shell's behavior to variations in its composition, providing valuable insights for applications where one side is clamped and the others are left free.

FGM Shell with Cut Sections

In Figure 5, the investigation expands to FGM shells with a doubled thickness of 40 mm while maintaining the same center cut sections, boundary conditions, and power law indexes (0.5, 1, 2, 5, 10). The results highlight the impact of increased thickness on natural frequencies, providing insights into how structural stiffness evolves with varying thickness for different geometric configurations. The study encompasses rectangular, square, and circular center cut sections under different boundary conditions ("CCCC," "CCFF," "CFFF"). Notably, the clamped boundary condition consistently yields higher natural frequencies, suggesting a stiffer structural response compared to other boundary conditions. Additionally, an increase in the power law index leads to a reduction in natural frequencies across all cases.

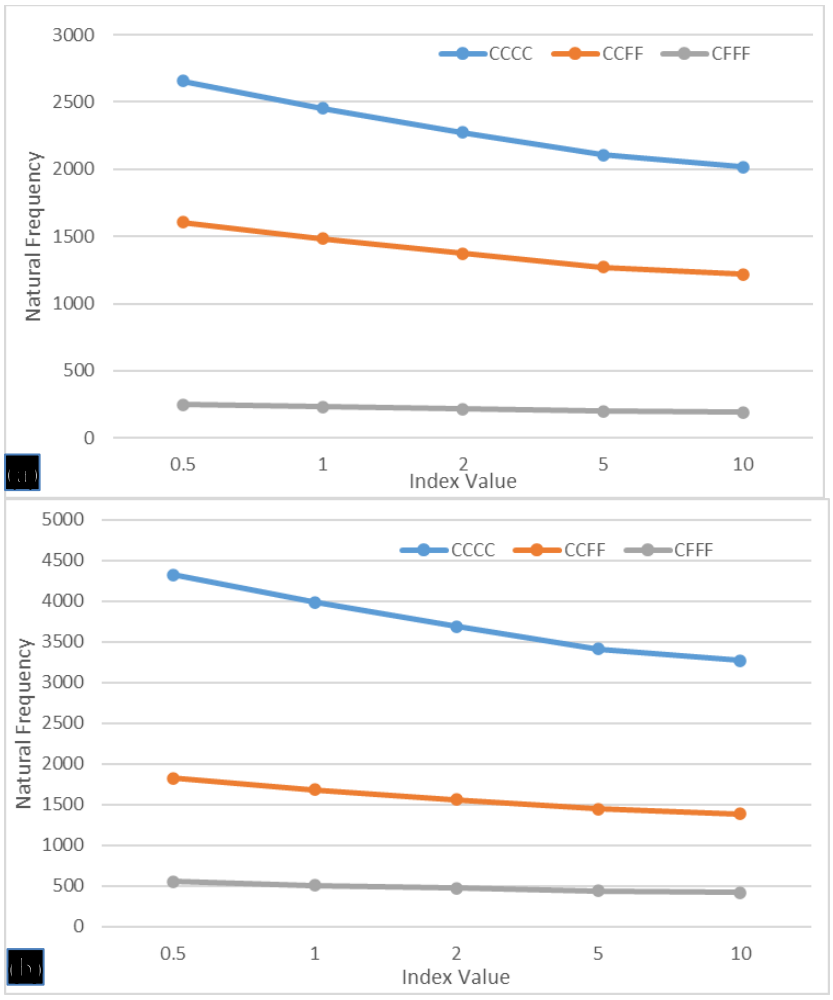

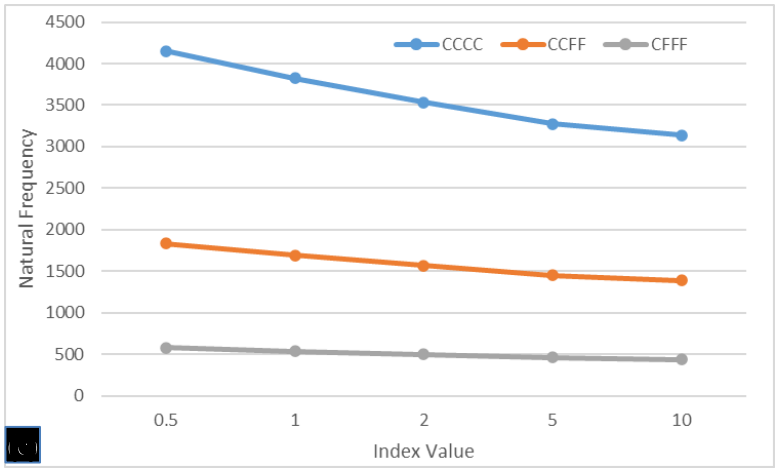

Figure 5. (a) Circular hole, (b) Square Hole, (c) Rectangular section. Variation of natural frequency of FGM shell with 20mm thickness centre cut section with various boundary conditions

Mode shapes of Natural Frequencies

These figures (6, 7, and 8) show how a hole in the center of a special material shell (FGM) affects how it vibrates. FGM shells have unique properties that change throughout their thickness. The pictures depict three different ways the shell can be clamped or held in place (fixed on all sides, two sides fixed and two free, or one side fixed and three free).

In all cases, the presence of the hole disrupts the normal vibration pattern of the shell. The way the shell vibrates (mode shape) depends on how it's clamped. For clamped edges, the movement is minimal near those edges, with more bending happening around the hole. Free edges, on the other hand, can move more freely. The exact shape of the hole (circle, rectangle, or square) also influences how the shell vibrates. These figures highlight that a hole in the center of an FGM shell significantly impacts how it vibrates, and this effect depends on both the hole shape and how the shell is clamped. Significantly, an intriguing revelation unfolds as identical FGM shell dimensions, with hole variations in the center hole cross-sectional design, yield disparate frequency outcomes. This phenomenon accentuates the pivotal role of the center cut section as a modulator of natural frequencies within the FGM shell. Especially, augmenting the power law index values intensifies this effect, systematically diminishing the frequencies across the diverse cut sections.

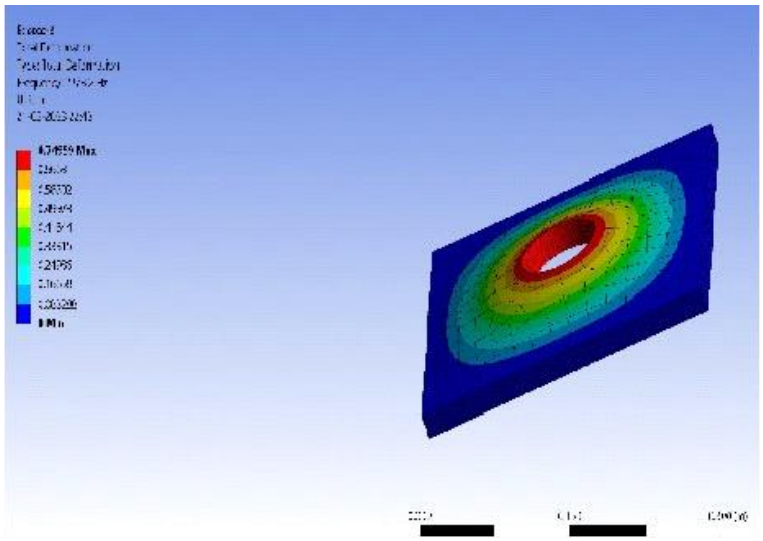

(a)All sides clamped, n=2, Mode 1

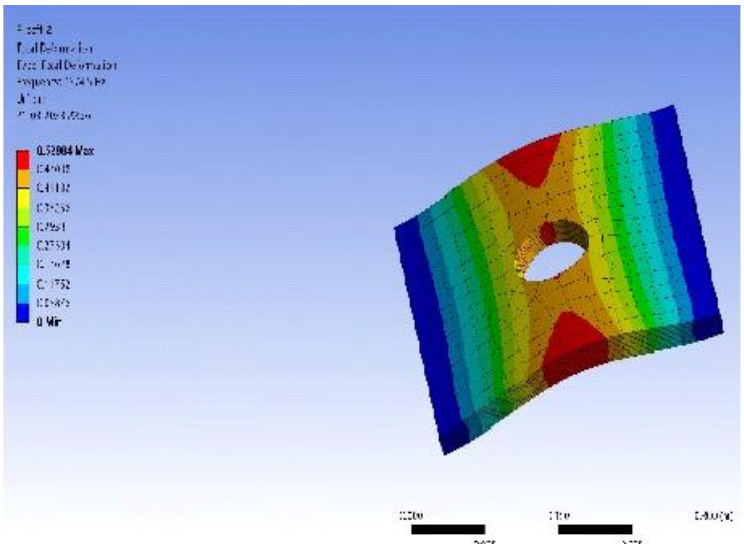

(b)Two sides clamped and two sides free n=2, Mode 1

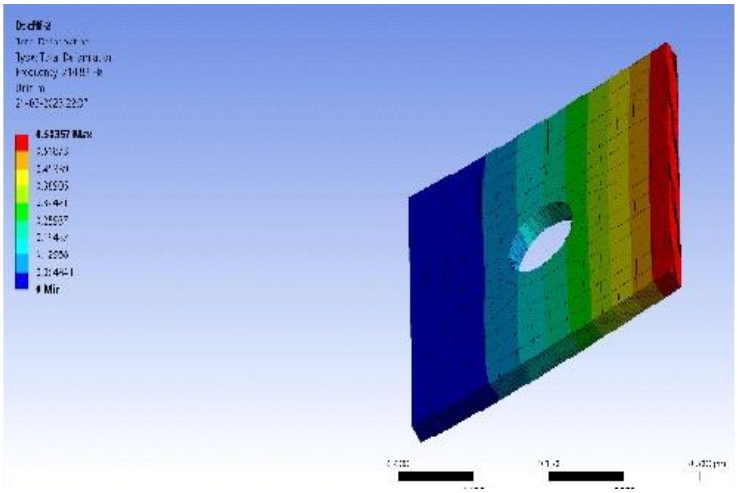

(c)One side clamped and three sides free, n=2, Mode 1

Figure 6. Mode Shapes of Natural Frequencies Circular Hole

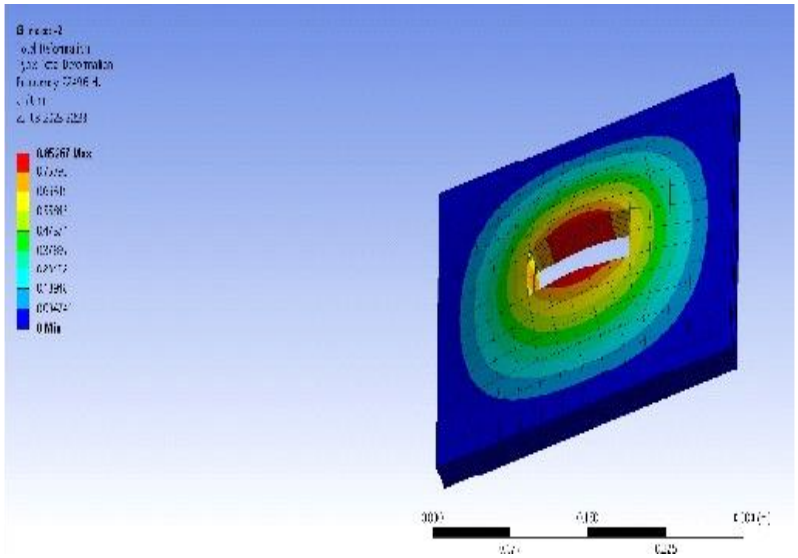

(a) All sides clamped, n=2, Mode 1

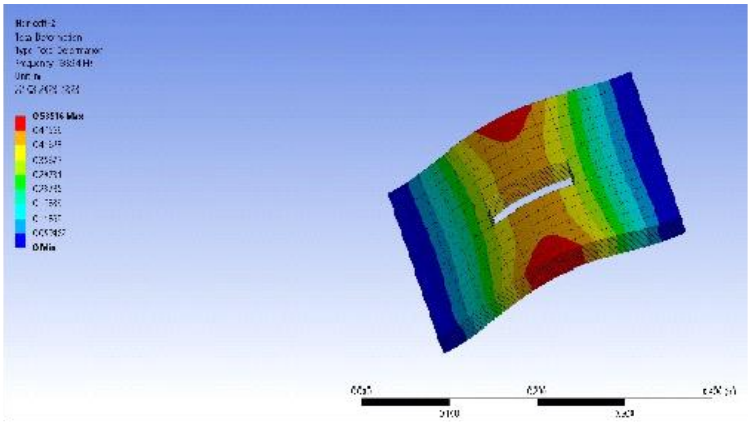

(b) Two sides clamped and two sides fixed, n=2, Mode 1

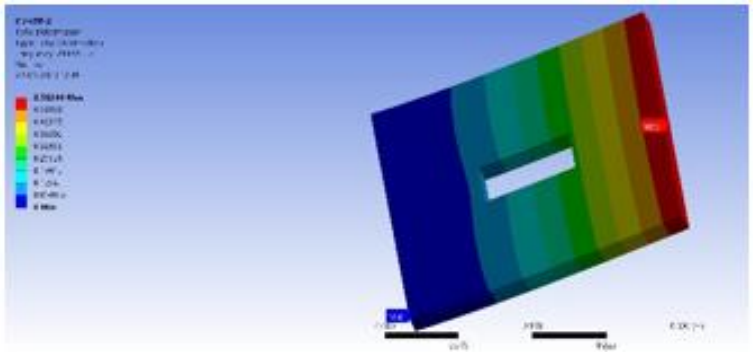

(c) One side clamped and three sides fixed, n=2, Mode 1

Figure7. Mode Shapes of natural frequencies rectangular hole.

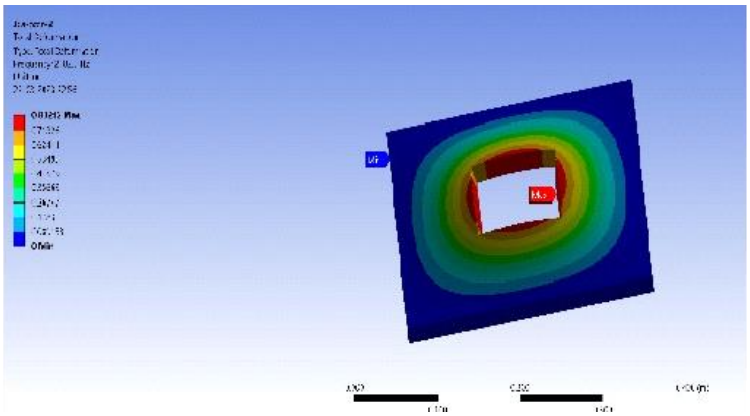

(a)All sides clamped, n=2, Mode 1

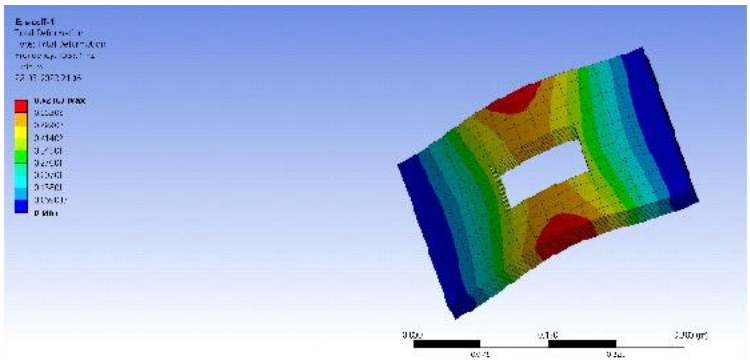

(b)Two sides clamped and two sides fixed, n=2, Mode 1

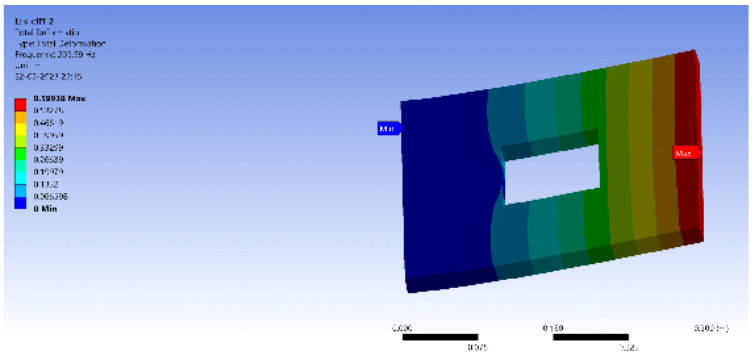

(c)One side clamped and three sides fixed, n=2, Mode 1

Figure 8. Mode shapes of natural frequencies square hole.

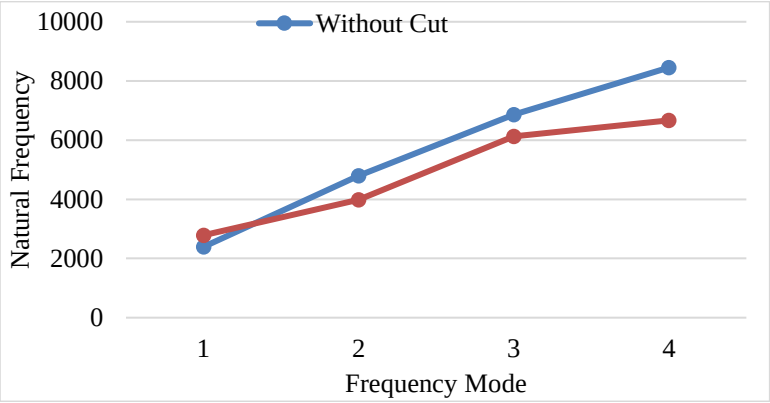

(a) CCCC

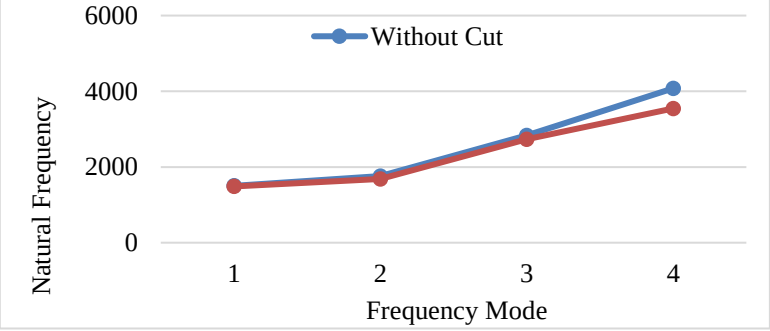

(b) CCFF

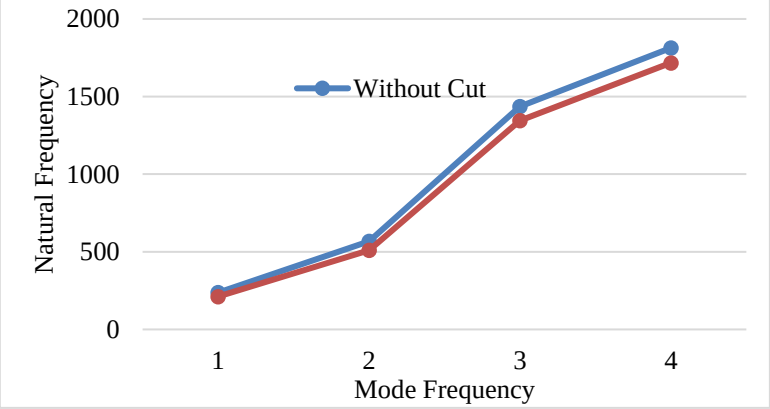

(c) CFFF

Figure 9. Comparison of first four mode natural frequency without and with centre square cut section

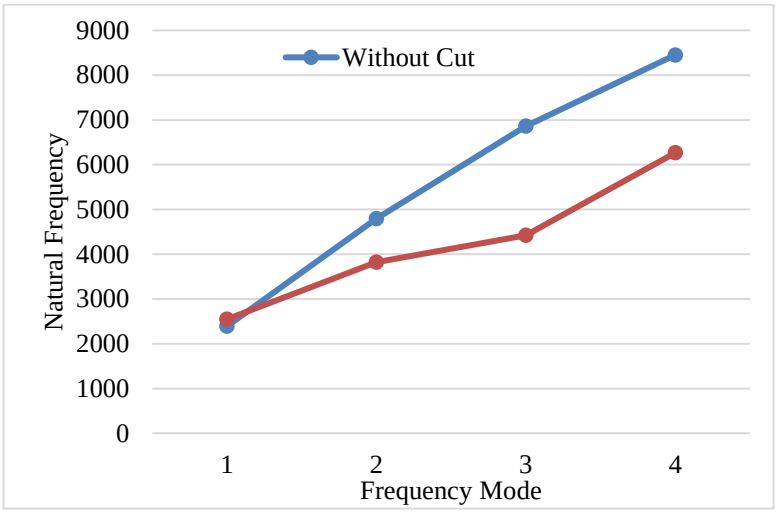

a) CCCC

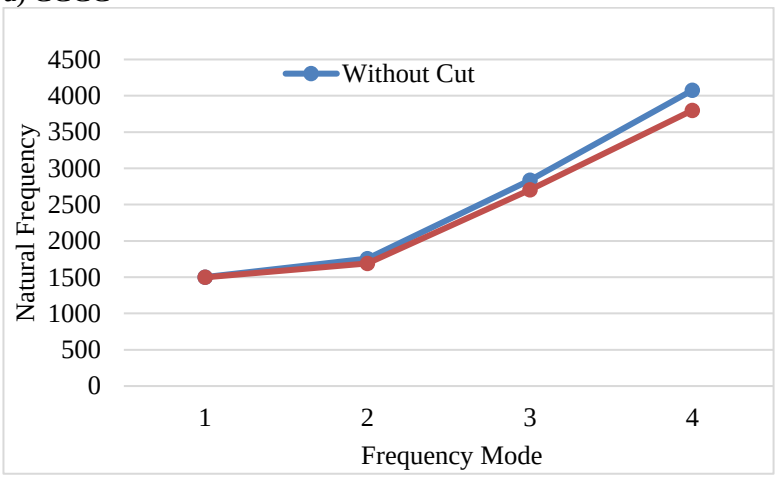

b) CCFF

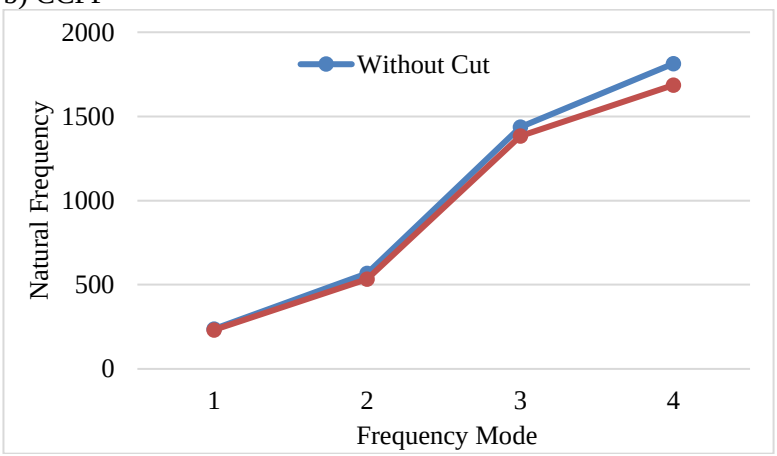

c) CFFF

Figure 10. Comparison of first four mode natural frequency without and with centre rectangle cut section.

The figure 9, 10 and 11 offer a visual exploration into the vibrational dynamics of square shells under varying boundary conditions and with central holes of different shapes—rectangular, circular, and square. Under the scenario where all sides of the shell are fixed, a clear trend emerges: the presence of a central hole consistently leads to higher bending frequencies compared to a solid shell without a hole.

This phenomenon is evident across all hole shapes depicted in the figures 9-11. Conversely, when considering torsional frequencies, the situation is reversed: the solid shell without a hole exhibits higher torsional frequencies compared to shells with central holes. This trend holds true regardless of the shape of the central hole. Moving to different boundary conditions, such as when two sides are fixed and two sides are free, or when one side is fixed and the other three sides are free, a consistent pattern emerges once again: both bending and torsional frequencies are lower for shells with central holes compared to solid plates without holes. This pattern remains consistent across all depicted boundary conditions and hole shapes. Ultimately, the figures 9-11 underscore the significance of central holes in influencing the vibrational behavior of square shells, with shells featuring central holes and fixed boundary conditions demonstrating notably heightened bending and torsional frequencies compared to other configurations.

The figure 9, 10 and 11 offer a visual exploration into the vibrational dynamics of square shells under varying boundary conditions and with central holes of different shapes—rectangular, circular, and square. Under the scenario where all sides of the shell are fixed, a clear trend emerges: the presence of a central hole consistently leads to higher bending frequencies compared to a solid shell without a hole. This phenomenon is evident across all hole shapes depicted in the figures 9-11. Conversely, when considering torsional frequencies, the situation is reversed: the solid shell without a hole exhibits higher

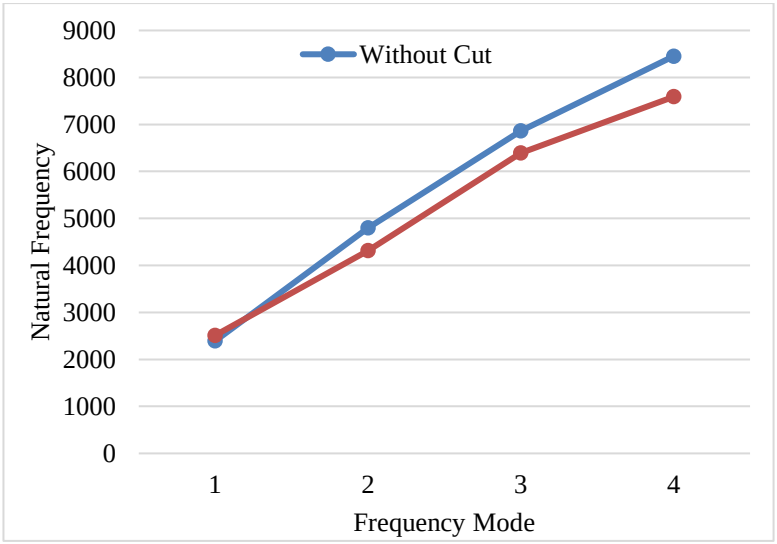

a) CCCC

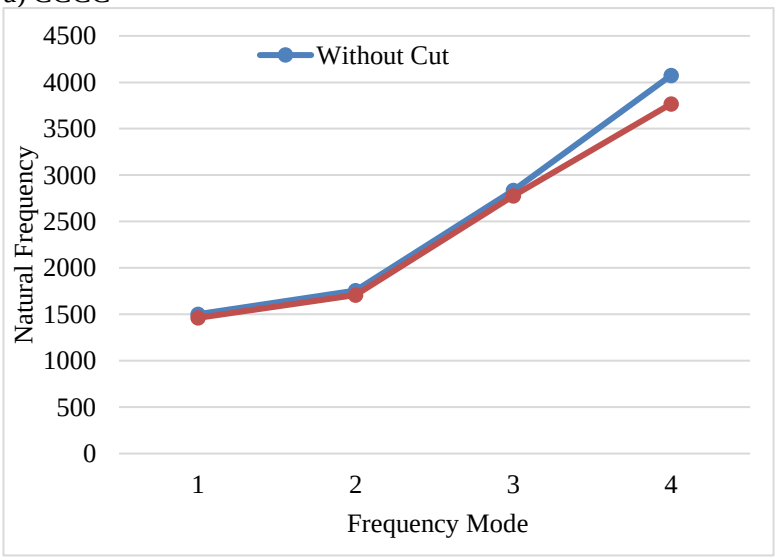

b) CCFF

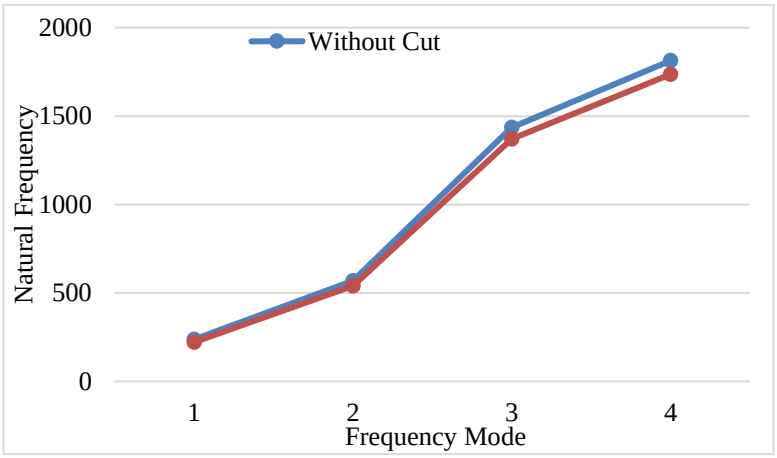

c) CFFF

Figure 11. Comparison of first four mode natural frequency without and with centre circle cut section

torsional frequencies compared to shells with central holes. This trend holds true regardless of the shape of the central hole. Moving to different boundary conditions, such as when two sides are fixed and two sides are free, or when one side is fixed and the other three sides are free, a consistent pattern emerges once again: both bending and torsional frequencies are lower for shells with central holes compared to solid plates without holes. This pattern remains consistent across all depicted boundary conditions and hole shapes. Ultimately, the figures 9-11 underscore the significance of central holes in influencing the vibrational behavior of square shells, with shells featuring central holes and fixed boundary conditions demonstrating notably heightened bending and torsional frequencies compared to other configurations.

CONCLUSIONS

Modal design and developed in Ansys Parametric Design Language (APDL) using shell element and designed the FGM material for this shell assigned to it. This FGM shell has been designed with the aid of a macro and is comprised of ten layers. Aluminium Oxide (Al_2O_3) is considered to be a ceramic material in this study, whereas stainless steel is considered to be a metal material. By applying Power Law and calculated Young's Modulus, Density, and Poison's Ratio for each layer for different power law indices i.e. 0.5,1,2,5,10. ANSYS simulations indicate that the value of natural frequencies increases with a higher thickness of the FGM plate under different boundary conditions, such as CCCC, CCFF, and CFFF. It can also be concluded that the value of natural frequencies decreases as the power law index increases. The boundary conditions also influence the change in natural frequencies. The shell without cut sections natural frequencies are less compared with cut section. Particularly, the square cut section natural frequencies are higher compared to with the circular and rectangular cut sections. The study highlights the critical role of boundary conditions and hole presence in dictating the vibrational behavior of FGM shells. Specifically, the clamped all sides configuration emerges as the most conducive to achieving high bending and torsional frequencies, emphasizing the necessity of tailored structural designs considering both geometric and boundary constraints.

REFERENCES

1. Naebe M, Shirvanimoghaddam. Functionally Graded Materials: A review of fabrication and properties. Materials Today 2016, 5: 223-245p.
2. Ramu I and Mohanty SC. Modal analysis of functionally graded material plates using finite element method. Procedia Materials Science 2014, 6: 460-7p.
3. Ramu I and Mohanty SC. Buckling analysis of rectangular functionally graded material plates under uniaxial and biaxial compression load. Procedia Engineering 2014, 86: 748-757p.
4. Rao DK, Blessington PJ, Tarapada R. Finite element modelling and analysis of functionally graded (FG) composite shell structures. Procedia Engineering, 2012, 38:3192-9p.
5. Sharma AK, Sharma P, Chauhan PS, et al. Study on harmonic analysis of functionally graded plates

using FEM. Int J Applied Mechanics and Engineering, 2018, 23(4):941-961p.
6. Ghassabi AA. Free vibration analysis of functionally graded rectangular nano-plates considering spatial variation of the non-local parameter. MSc Thesis, Middle East Technical University, Turkey, 2017.
7. Ramu I and Mohanty SC. Free Vibration and Dynamic Stability of Functionally Graded Material Plates on Elastic Foundation. Defence Science Journal 2015, 65, no. 3, pp. 245-251p.
8. Bhandari M, Purohit K. Analysis of functionally graded material plate under transverse load for various boundary conditions. IOSR Journal of Mechanical and Civil Engineering 2014, 10(5): 46-55p.
9. Alif Ngimbi Diambu and Mehmet Çevik. Finite element analysis of a functionally graded plate. Third International Students Science Congress Proceedings, ,2019: 517-523p.
10. Alif Ngimbi Diambu and Mehmet Çevik. Finite Element Vibration Analysis of a Functionally Graded Plate, 5th International Students Science Congress Proceedings, 2021,332-344p.
11. Tawakol AE. Stress concentration analysis in functionally graded plates with elliptic holes under biaxial loadings. AinShams EngineeringJournal5 2014, (3):839-850p.
12. Ramu Inala. Influence of Hygrothermal Environment and FG Material on Natural Frequency and Parametric Instability of Plates. Mechanics of Advanced Composite Structures, 2020, 7(1): 89-101p.
13. Merdaci S, Mostefa AH, Merazi M, et al. Free vibration analysis of ceramic-metal functionally graded rectangular solar plates with porosities using high-order shear theory: Solar plate FG composed of (Al/Al2O3) and (Al/ZrO2) influence by porosity. 11thInternational Renewable Energy Congress (IREC), 2020.
14. Liew KM, Kitipornchai S Leung, AYT, et al. Analysis of the free vibration of rectangular plates with central cut-outs using the discrete Ritz method. International Journal of Mechanical Sciences, 2003, 45: 941–959p.
15. Kanak Kalita, Salil Haldar. Free vibration analysis of rectangular plates with central cutout. Cogent Engineering, .2016, 3(1),1163781p.
16. Anjibabu Merneedi, Mohan Rao Nalluriand, Subba Rao VV. Free vibration analysis of a thin rectangular plate with multiple circular and rectangular cut-outs, Journal of Mechanical Science and Technology, 2017, 31: 5185–5202p.
17. Khudhayer J Jadee, Balsam H Abed, Ali Adel Battawi. Free vibration of isotropic plates with various cutout configurations using finite elements and design of experiments. IOP Conference Series: Materials Science and Engineering, 2020, 745, 012080p.
18. Lee HL, Lim SP, & Chow ST. Prediction of natural frequencies of rectangular plates with rectangular cutouts. Computers and Structures, 1990, 36: 861–9p.
19. Torabi K and Azadi AR. Vibration analysis for rectangular plate having a circular central hole with point support by Rayleigh-Ritz method, Journal of Solid Mechanics, 2014, 6 (1): 28–42p.

